Inorg. Chem. **2003**, *42*, 7912–7920

Geometry-Dependent Phosphodiester Hydrolysis Catalyzed by Binuclear Copper Complexes

Lei Zhu, Osvaldo dos Santos, Chi Wan Koo, Marc Rybstein, Louise Pape, and James W. Canary*

Department of Chemistry, New York University, New York, New York 10003

Received January 29, 2003

Two isomeric binuclear ligands **PBTPA** and **MBTPA** and their copper(II) complexes were prepared and examined for hydrolysis of a model phosphodiester substrate: bis(*p*-nitrophenyl)phosphate. A bell-shaped pH vs rate profile, which is in agreement with one mechanism proposed for bimetallonucleases/phosphatases, was observed for the binuclear complex of copper(II) and **PBTPA**. At pH 8.4, a maximum rate of 1.14×10^{-6} s^{-1}—more than 10^4-fold over uncatalyzed reactions—was achieved. However, the analogous complex of **MBTPA** did not show significant rate enhancement. The binuclear complex of copper(II) and **PBTPA** also showed 10-fold acceleration over mononuclear complex of copper(II) and tris(2-pyridylmethyl)amine (**TPA**) catalyzed reaction. A phage ϕX174 DNA assay showed that the complex of copper(II) and **PBTPA** promoted supercoiled phage ϕX174 DNA relaxation under both aerobic and anaerobic conditions, in contrast to the hydrolytic inactivity of the mononuclear complex of copper(II) and **TPA**.

Introduction

The remarkable stability of the DNA phosphodiester backbone is one of the essential requirements for the survival and maintenance of life.[1] The half-life for hydrolytic cleavage of a typical DNA phosphodiester bond at 25 °C in neutral water is estimated to be on the order of billions of years.[2] On the other hand, the stability of the DNA phosphodiester backbone provides a daunting task for scientists who wish to engineer DNA structure, including specific cleavage and ligation, to achieve desired functions.[3] However, enzymes such as polymerases, recombinases, topoisomerases, reverse transcriptases, and others catalyze phosphoryl transfer reactions efficiently under physiological conditions. Many such enzymes include nuclease motifs with metal-ion-containing active sites,[4,5] which represent the structural basis for biomimetic simulation.[6]

An array of coordination compounds of transition metal ions[7−37] and lanthanide ions[38−42] has been reported to catalyze hydrolysis of nucleic acid backbones or phosphodiester model systems to various degrees.[43−47] Among these, Cu-

* To whom the correspondence should be addressed. E-mail: james.canary@nyu.edu. Fax: (212) 260 7905.

(1) Westheimer, F. H. *Science* **1987**, *235*, 1173.
(2) Williams, N. H.; Takasaki, B.; Wall, M.; Chin, J. *Acc. Chem. Res.* **1999**, *32*, 485.
(3) Hegg, E. L.; Burstyn, J. N. *Coord. Chem. Rev.* **1998**, *173*, 133.
(4) Sträter, N.; Lipscomb, W. N.; Klabunde, T.; Krebs, B. *Angew. Chem., Int. Ed. Engl.* **1996**, *35*, 2024.
(5) Wilcox, D. E. *Chem. Rev.* **1996**, *96*, 2435.
(6) Bashkin, J. K. *Chem. Rev.* **1998**, *98*, 937.
(7) For examples of hydrolyses of RNA/RNA model systems by metal complexes, see the following and refs 8−18. Iranzo, O.; Kovalevsky, A. Y.; Morrow, J. R.; Richard, J. P. *J. Am. Chem. Soc.* **2003**, *125*, 1988.
(8) Kawahara, S.-I.; Uchimaru, T. *Eur. J. Inorg. Chem.* **2001**, 2437.
(9) Ait-Haddou, H.; Sumaoka, J.; Wiskur, S. L.; Folmer-Andersen, J. F.; Anslyn, E. V. *Angew. Chem., Int. Ed.* **2002**, *41*, 4014.
(10) Worm, K.; Chu, F.; Matsumoto, K.; Best, M. D.; Lynch, V.; Anslyn, E. V. *Chem. Eur. J.* **2003**, *9*, 741.
(11) Matsuda, S.; Ishikubo, A.; Kuzuya, A.; Yashiro, M.; Komiyama, M. *Angew. Chem., Int. Ed.* **1998**, *37*, 3284.
(12) Rossi, P.; Felluga, F.; Tecilla, P.; Formaggio, F.; Crisma, M.; Toniolo, C.; Scrimin, P. *J. Am. Chem. Soc.* **1999**, *121*, 6948.
(13) He, C.; Lippard, S. J. *J. Am. Chem. Soc.* **2000**, *122*, 184.
(14) Young, M. J.; Chin, J. *J. Am. Chem. Soc.* **1995**, *117*, 10577.
(15) Liu, S.; Hamilton, A. D. *Bioorg. Med. Chem. Lett.* **1997**, *7*, 1779.
(16) Liu, S.; Hamilton, A. D. *Chem. Commun.* **1999**, 587.
(17) McCue, K. P.; Morrow, J. R. *Inorg. Chem.* **1999**, *38*, 6136.
(18) Fritsky, I. O.; Ott, R.; Kramer, R. *Angew. Chem., Int. Ed.* **2000**, *39*, 3255. For examples of hydrolyses of DNA/DNA model systems by metal (except copper(II)) complexes, see refs 19−27.
(19) Hettich, R.; Schneider, H.-J. *J. Am. Chem. Soc.* **1997**, *119*, 5638.
(20) Schnaith, L. M. T.; Hanson, R. S.; Que, L. J. *Proc. Natl. Acad. Sci. U.S.A.* **1994**, *91*, 569.
(21) Vichard, C.; Kaden, T. *Inorg. Chim. Acta* **2002**, *337*, 173.
(22) Gultneh, Y.; Khan, A. R.; Blaise, D.; Chaudhry, S.; Ahvazi, B.; Marvey, B. B.; Butcher, R. J. *J. Inorg. Biochem.* **1999**, *75*, 7.
(23) Jurek, P.; Martell, A. E. *Inorg. Chim. Acta* **1999**, *287*, 47.
(24) Bencini, A.; Berni, E.; Bianchi, A.; Fedi, V.; Giorgi, C.; Paoletti, P.; Valtancoli, B. *Inorg. Chem.* **1999**, *38*, 6323.
(25) Chapman, W. H.; Breslow, R. *J. Am. Chem. Soc.* **1995**, *117*, 5462.
(26) Leivers, M.; Breslow, R. *Bioorg. Chem.* **2001**, *29*, 345.
(27) Kondo, S.-I.; Shinbo, K.; Yamaguchi, T.; Yoshida, K.; Yano, Y. *J. Chem. Soc., Perkin Trans. 2* **2001**, 128.

10.1021/ic0340985 CCC: $25.00
Published on Web 11/06/2003

Chart 1 [a]

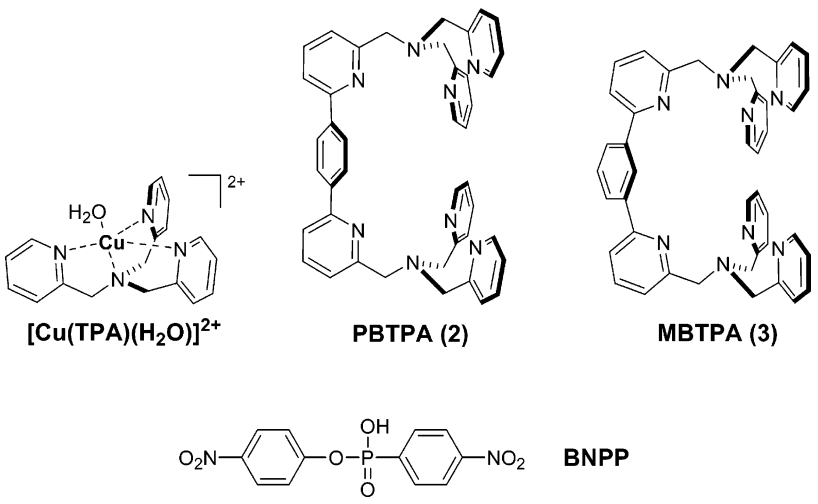

[a] Mononuclear Cu(II) complex [Cu(II)(**TPA**)(H_2O)]$^{2+}$; binuclear ligands **2** and **3**; bis(*p*-nitrophenyl)phosphate (**BNPP**).

(II) complexes have been studied extensively in the past decade in promoting hydrolyses of DNA or model substrates,[3,28−37] because of Cu(II) ion's similar coordination chemistry and usually superior Lewis acidity to that of Zn(II), which has been observed as cofactor in many nucleases.[4,5]

On the other hand, nucleic acid hydrolysis by many metallonucleases/phosphatases is postulated to be facilitated frequently by the cooperative action of two metal ions in their active sites,[4] with one metal ion activating the phosphodiester substrate, and the other increasing the pK_a of the bound water.[5] Therefore, in a biomimetic two-metal-ion system,[2,48,49] one coordinated metal ion should be engineered to bind a water ligand which ionizes to generate a hydroxide nucleophile under physiological conditions. The other metal ion would bind with phosphoryl oxygen atoms in the substrate to neutralize the developing negative charges in the transition state structures. The two coordination domains should be connected by a suitable linker so that the intermetal distance as well as the overall geometry of the binuclear center can be optimized to generate high hydrolytic activity toward given substrates. Therefore, binuclear, Cu(II)-containing complexes that feature appropriate geometries in regard to the two metal binding sites would likely possess nuclease activity in a biomimetic fashion[34] (Chart 1).

The ligand tris(2-pyridylmethyl)amine (**TPA**, **1**) is known to form stable complexes with metal ions of small atomic radii (∼0.8 Å) such as Zn(II) and Cu(II).[50] In aqueous solution, [Zn(**1**)OH_2]$^{2+}$ displays an acidic water molecule with pK_a 8.0[50] and does not aggregate under high-pH conditions.[51] A binuclear metal complex containing [Zn(II)(**TPA**)] motif has already been reported to be capable of promoting hydrolysis of bis(*p*-nitrophenyl)phosphate (**BNPP**).[52] The pK_a of [Cu(**1**)OH_2]$^{2+}$ is ∼7.4,[50] which is acidic enough to be deprotonated under near physiological conditions to provide a metal ion bound hydroxide nucleophile. In this Article, we first studied the coordination chemistry between [Cu(**1**)]$^{2+}$ and the model phosphodiester compound **BNPP** in an effort to validate that [Cu(II)(**TPA**)] domain binds a phosphodiester substrate in a fashion similar to what is observed in metallonuclease−substrate complexes. Second, binuclear ligands and complexes were prepared by connecting two **TPA** motifs with proper spacers. Last, structural and kinetics studies were performed with selected binuclear coordination complexes.

(28) DNA/DNA model system hydrolyses by mononuclear copper(II) complexes: the following and refs 29−33. Sreedhara, A.; Cowan, J. A. *Chem. Commun.* **1998**, 1737.
(29) Sreedhara, A.; Freed, J. D.; Cowan, J. A. *J. Am. Chem. Soc.* **2000**, *122*, 8814.
(30) Ren, R.; Yang, P.; Zheng, W.; Hua, Z. *Inorg. Chem.* **2000**, *39*, 5454.
(31) Hegg, E. L.; Mortimore, S. H.; Cheung, C. L.; Huyett, J. E.; Powell, D. R.; Burstyn, J. N. *Inorg. Chem.* **1999**, *38*, 2961.
(32) Deck, K. M.; Tseng, T. A.; Burstyn, J. N. *Inorg. Chem.* **2002**, *41*, 669.
(33) Itoh, T.; Hisada, H.; Sumiya, T.; Hosono, M.; Usui, Y.; Fujii, Y. *J. Chem. Soc., Chem. Commun.* **1997**, 677.
(34) DNA/DNA model system hydrolyses by binuclear copper(II) complexes: the following and refs 35−37. Molenveld, P.; Engbersen, J. F. J.; Kooijman, H.; Spek, A. L.; Reinhoudt, D. N. *J. Am. Chem. Soc.* **1998**, *120*, 6726.
(35) De Iuliis, G.; Lawrance, G. A.; Fieuw-Makaroff, S. *Inorg. Chem. Commun.* **2000**, *3*, 307.
(36) Gajda, T.; Dupre, Y.; Torok, I.; Harmer, J.; Schweiger, A.; Sander, J.; Kuppert, D.; Hegetschweiler, K. *Inorg. Chem.* **2001**, *40*, 4918.
(37) Rossi, L. M.; Neves, A.; Horner, R.; Terenzi, H.; Szpoganicz, B.; Sugai, J. *Inorg. Chim. Acta* **2002**, *337*, 366.
(38) Wang, C.; Choudhary, S.; Vink, C. B.; Secord, E. A.; Morrow, J. R. *Chem. Commun.* **2000**, 2509.
(39) Epstein, D. M.; Chappell, L. L.; Khalili, H.; Supkowski, R. M.; Horrocks, W. D., Jr.; Morrow, J. R. *Inorg. Chem.* **2000**, *39*, 2130.
(40) Welch, J. T.; Sirish, M.; Lindstrom, K. M.; Franklin, S. J. *Inorg. Chem.* **2001**, *40*, 1982.
(41) Branum, M. E.; Tipton, A. K.; Zhu, S.; Que, L. J. *J. Am. Chem. Soc.* **2001**, *123*, 1898.
(42) Kim, Y.; Franklin, S. J. *Inorg. Chim. Acta* **2002**, *341*, 107.
(43) Representative reviews on metal complex catalyzed nucleic acid/model system hydrolyses: the following and refs 44−49. Franklin, S. J. *Curr. Opin. Chem. Biol.* **2001**, *5*, 201.
(44) Ott, R.; Kramer, R. *Appl. Microbiol. Biotechnol.* **1999**, *52*, 761.
(45) Bashkin, J. K. *Curr. Opin. Chem. Biol.* **1999**, *3*, 752.
(46) Sreedhara, A.; Cowan, J. A. *J. Biol. Inorg. Chem.* **2001**, *6*, 337.
(47) Cowan, J. A. *Curr. Opin. Chem. Biol.* **2001**, *5*, 634.
(48) Chin, J. *Curr. Opin. Chem. Biol.* **1997**, *1*, 514.
(49) Molenveld, P.; Engbersen, J. F. J.; Reinhoudt, D. N. *Chem. Soc. Rev.* **2000**, *29*, 75.
(50) Anderegg, G.; Hubmann, E.; Podder, N. G.; Wenk, F. *Helv. Chim. Acta* **1977**, *60*, 123.
(51) Chiu, Y.-H.; Canary, J. W. *Inorg. Chem.* **2003**, *42*, 5107−16.
(52) dos Santos, O.; Lajmi, A. R.; Canary, J. W. *Tetrahedron Lett.* **1997**, *38*, 4383.

Experimental Details

General. All reactions were performed in oven-dried glassware under an atmosphere of argon gas. ^{1}H NMR and ^{13}C NMR were recorded on a Varian-Gemini 200 MHz spectrometer. FAB mass spectra were measured using the matrix NBA/$CHCl_3$. ESI mass spectra were measured with a PE SCIEX API electrospray LC/MS spectrometer. Compounds **TPA**[53] (**1**) and **BrTPA**[54] (**4**) were prepared by literature procedures.

[Cu(1)(BNPP)](ClO_4). (***CAUTION!*** Perchlorate salts of metal complexes with organic ligands are potentially explosive. They should be handled in small quantity and with caution.)[55] Tris(2-pyridylmethyl)amine (**TPA**, **1**, 73 mg, 0.25 mmol), $Cu(ClO_4)_2 \cdot 6H_2O$ (93 mg, 0.25 mmol), and bis(*p*-nitrophenyl)phosphate (**BNPP**, 85 mg, 0.25 mmol) were dissolved in MeOH (2.0 mL). To this methanolic solution, NaOH (1.0 M) was added dropwise until the pH reached 6. The solution was warmed to 50 °C. DMSO was added in the heated solution dropwise with stirring until the precipitate disappeared. The clear solution was allowed to stand at room temperature overnight while blue crystals of [Cu(**1**)(**BNPP**)](ClO_4) were formed at the bottom of the container (124 mg, 65%). The product was redissolved in CH_3CN. The crystals suitable for X-ray structure determination were grown by Et_2O diffusion into its CH_3CN solution over 48 h. MS (ESI): calcd (M^+) 692.09, found 692.

PBTPA (2). To a solution of **BrTPA** (**4**, 369 mg, 1 mmol), 1,4-benzene diboronic acid (**5**, 82 mg, 0.5 mmol), and $Pd(PPh_3)_4$ (173 mg, 0.15 mmol) in toluene (3.0 mL) and MeOH (2.0 mL) was added aqueous Na_2CO_3 (3.0 mL, 2 M). The solution was stirred at reflux for 16 h. After the reaction mixture was cooled, 5% HCl was added dropwise until pH reached ~1. The mixture was stirred for another 30 min. The crude product was diluted with H_2O to 50 mL and extracted with Et_2O (2 × 50 mL). The aqueous layer was basified carefully with 10% NaOH to pH > 10 and extracted with CH_2Cl_2 (3 × 50 mL). The combined organic fractions were collected and dried over Na_2SO_4. Evaporation of the solvent under reduced pressure gave the residue, which was chromatographed on alumina gel with MeOH/CH_2Cl_2 (from 0/100 to 1.5/100) as eluant to give the pure product (438 mg). The yield was 67%. ^{1}H NMR (200 MHz, $CDCl_3$): δ 8.54 (d, 4H, J = 4.0 Hz), 8.13 (s, 4H), 7.8−7.5 (m, 14H), 7.13−7.17 (m, 4H), 3.97 (s, 12H). ^{13}C NMR (50 MHz, $CDCl_3$): δ 159.9, 156.6, 149.6, 149.5, 140.2, 137.5, 136.8, 127.7, 123.4, 122.4, 121.9, 119.2, 60.8, 60.7. MS (FAB): calcd ($M + H^+$) 655.32, found 655.65. Anal. Calcd for $C_{42}H_{38}N_8$: C, 77.04; H, 5.85; N, 17.11. Found: C, 76.96; H, 5.93; N, 17.05.

MBTPA (3). MBTPA was prepared by Suzuki reaction between **4** and 1,3-benzene diboronic acid dipinacol ester (**6**) by the procedure applied to **2** above. The crude product was chromatographed on silica gel with MeOH/CH_2Cl_2 (from 0/100 to 2/100) in the presence of 1% triethylamine to yield 278 mg of product. The yield was 85%. ^{1}H NMR (200 MHz, $CDCl_3$): δ 8.63 (t, 1H, J = 1.5 Hz), 8.56−8.50 (m, 4H), 8.06 (dd, 2H, J = 1.7, 7.8 Hz), 7.80−7.50 (m, 15H), 7.13 (m, 4H), 3.97 (s, 12H). ^{13}C NMR (50 MHz, $CDCl_3$): δ 160.1, 159.8, 157.0, 149.6, 140.4, 137.6, 136.9, 129.6, 127.9, 126.0, 123.4, 122.4, 121.7, 119.3 60.8. MS (MALDI-TOF): calcd ($M + H^+$) 655.32, found 655.9. Anal. Calcd for $C_{42}H_{40}N_8O$ (**3**·H_2O): C, 74.98; H, 5.99; N, 16.65. Found: C, 74.64; H, 5.80; N, 16.86.

[Zn_2(2)($AN)_2$](ClO_4)$_4$ (7). (***CAUTION!*** Perchlorate salts of metal complexes with organic ligands are potentially explosive. They should be handled in small quantity and with caution.)[55] $Zn(ClO_4)_2 \cdot 6H_2O$ (37 mg, 0.1 mmol) in MeOH (1.0 mL) and **BPTPA** (**2**, 33 mg, 0.05 mmol) in CH_3CN (1.0 mL) were mixed together. The mixture was heated until a homogeneous solution was formed. Most of the solvent was then removed under vacuum so that the complex (Zn_2(**2**)(H_2O)$_2$(ClO_4)$_4$, 56 mg, 92%) was precipitated and collected by filtration. Anal. Calcd for $C_{42}H_{42}Cl_4N_8O_{18}Zn_2$: C, 41.37; H, 3.47; N, 9.19. Found: C, 41.39; H, 3.54; N, 8.85. Crystals suitable for X-ray diffraction were prepared by diffusing various volatile solvents into the CH_3CN solution of the complex. Colorless transparent crystals were obtained respectively with Et_2O, THF, EtOAc, and CH_2Cl_2 as diffusing solvents. The crystals prepared from Et_2O (**7a**) and THF (**7b**) diffusion were submitted for X-ray structural determination.

[Cu_2(2)($AN)_2$](ClO_4)$_4$ (8). (***CAUTION!*** Perchlorate salts of metal complexes with organic ligands are potentially explosive. They should be handled in small quantity and with caution.)[55] $Cu(ClO_4)_2 \cdot 6H_2O$ (37 mg, 0.1 mmol) in MeOH (1.0, mL) and **BPTPA** (**2**, 33 mg, 0.05 mmol) in CH_3CN (1.0 mL) were mixed together. A blue precipitate appeared immediately. Most of the solvent was removed under vacuum, and the bluish powdery complex (Cu_2(**2**)($AN)_2$(ClO_4)$_4$, 60 mg, 95%) was collected by filtration. Anal. Calcd for $C_{46}H_{44}Cl_4Cu_2N_{10}O_{16}$: C, 43.79; H, 3.51; N, 11.10. Found: C, 43.64; H, 3.19; N, 10.93. Pleochroic (blue and violet) transparent crystals in clusters (4−6 pieces/cluster) were obtained when EtOAc diffused in the CH_3CN solution of the complex.

Kinetic Measurements. Spectrophotometric grade DMSO was used. All buffers were prepared with deionized H_2O. The pH of each solution was measured with a Mettler Toledo Inlab electrode (Ag/AgCl reference) and an Accumet pH meter 10 at room temperature at the end of each kinetic run. The free acids of HEPES, EPPS, CHES, and CAPS (0.1 M with 0.2 M $NaClO_4$ each) were titrated to the desired pH with NaOH (1 M). All absorbance spectra were recorded with a PerkinElmer Lambda 40 UV/vis spectrometer fitted with a thermostated cuvette holder and sample transport accessory. Samples were prepared in 1 cm path length glass microcuvettes. Deionized water (160 μL), buffer (0.1 M, 500 μL), DMSO (220 μL), the substrate **BNPP** (50 mM in DMSO, 40 μL), binuclear ligand (5.0 mM in DMSO, 40 μL), and aqueous $Cu(ClO_4)_2$ (10.0 mM, 40 μL) solutions were measured into the cuvette sequentially to constitute a 30% DMSO solution. After 15 min equilibration time, the increase in concentration of *p*-nitrophenylate (λ = 400 nm) was measured every 100 s for 3 h. The initial slope (<5% conversion) of a plot of the measured absorbance vs time was determined (R^2 ($Cu(II)_2$(**2**)) > 0.999; R^2 ($Cu(II)_2$(**3**)) > 0.9) The rate constants were calculated with the extinction coefficient of *p*-nitrophenylate at 400 nm read from a pH−ϵ correlation curve for 30% DMSO solution at 55 °C. The experiment with mononuclear catalyst Cu(II)(**1**) was performed in a similar way while the mononuclear ligand (**TPA**, **1**) concentration was 10.0 mM instead of 5.0 mM.

Preparation of ϕX174 RFI DNA Solution. The EDTA in ϕX174 RFI DNA purchased from New England Biolabs was removed via ethanol precipitation followed by a 70% ethanol wash. The pellet was suspended in 10 mM Tris-Cl buffer (pH 8.0, no EDTA). The final concentration of the DNA solution was 0.1 μg/μL.

Aerobic Reaction with Cu(II) Complexes. The reaction mixture was prepared by adding $Cu(ClO_4)_2$ (2.0 μL, 50 mM), DMSO (2.0 μL), ligand **2** in DMSO (1.0 μL, 50 mM), the buffer (4.0 μL, 0.1 M CHES, 0.2 M $NaClO_4$, pH 8.75), and ϕX174 DNA (1.0 μL, 0.1 g/L) to sterile 1.5 mL Eppendorf tubes sequentially; in the experiments with no catalyst, with free Cu^{2+} or with mononuclear

(53) Toftlund, H.; Ishiguro, S. *Inorg. Chem.* **1989**, *28*, 2236.
(54) Chuang, C.-L.; dos Santos, O.; Xu, X.; Canary, J. W. *Inorg. Chem.* **1997**, *36*, 1967.
(55) *Chem. Eng. News* **1983**, *61*, 1 (Dec 5), 4.

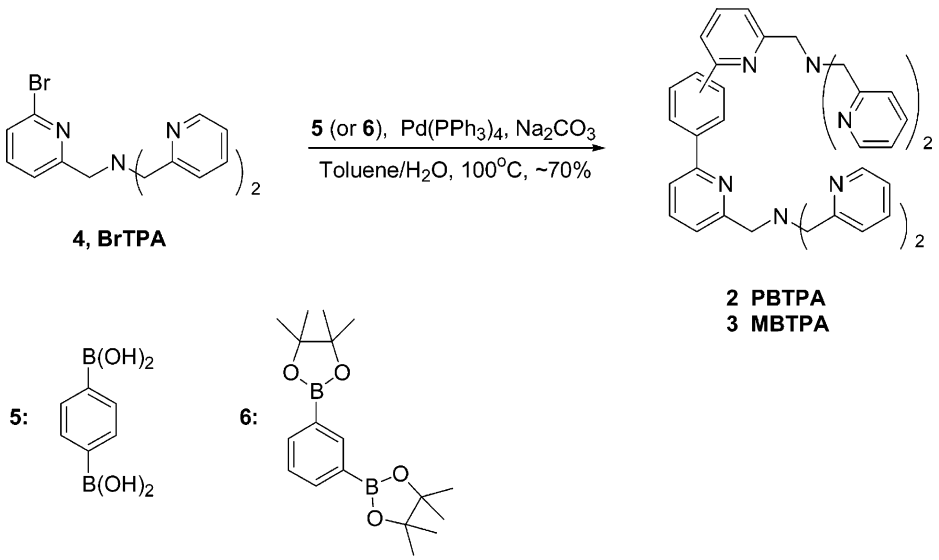

Figure 1. Synthesis of binuclear ligands **2** and **3**.

catalyst Cu(II)(**1**), the quantity of each added solution was adjusted so that the percentage of DMSO remained at 30%.The total volume was 10 μL. These mixtures were vortexed and centrifuged to facilitate the complexation of ligands with Cu(II) ions before the addition of ϕX174 DNA. The mixtures were then vortexed and centrifuged again to initiate the reactions. Then the solutions were incubated at 45 °C for 2 h. Immediately after incubation, 2 μL of EDTA solution were added to all reaction mixtures, followed by 5 min of incubation at 37 °C to minimize precipitation. The reaction mixtures were then quenched with 4 μL of FSM (purchased from Sigma) before loading onto an agarose gel (purchased from Bio-Rad). The DNA solutions were subjected to electrophoresis on a 1% agarose gel at either 22 mV in 1XTBE buffer solution (purchased from United States Biochemical) overnight for the 20 cm long gel, or at 65 mV for 2 h in the same buffer for the midigel. The gel was stained in 1 μg/mL ethidium bromide solution (purchased from United States Biochemical) for 10 min and destained for 2 h. The gel was photographed under UV light, and bands of the scanned image were quantified by "Intelligent Quantifier" software (RM Luton, Inc.).

Anaerobic Reaction with Cu(II) Complexes. Deoxygenated water, buffer, and DNA solutions were prepared by either three or four "freeze−pump−thaw" cycles. All solutions were stored under a nitrogen atmosphere prior to use. All anaerobic stock solutions were prepared in a nitrogen-filled inflatable polyethylene chamber with built-in gloves. A sealed atomsbag was purged with N_2 for 2 h prior to use. Reaction mixtures were prepared in the atomsbag by the addition of appropriate volumes of stock solutions to the reaction tubes. The procedure for mixing all reagents in the sterile Eppendorf tubes was the same as described for the aerobic reaction. Reactions between the complexes and DNA were initiated by quick centrifugation, transfer to a nitrogen-filled vacuum desiccator, and incubation in the sealed desiccator at 45 °C for 2 h. Procedures for treatment of the mixtures after incubation are the same as those described for the aerobic reaction.

Results and Discussion

Both compounds **PBTPA** (**2**) and **MBTPA** (**3**) contain two homogeneous N_4 binding sites linked together by phenyl linkers elaborated in such a fashion that both metal binding sites are either *para* (**2**) or *meta* (**3**) to each other. The intermetal distance in a bimetallic complex of **2** would be ~4 Å, on the basis of the examination of CPK molecular models, upon binding with a phosphodiester substrate, while in **3** the distance would be shorter. The phenyl linkers also provide some degree of rotational freedom so that they would accommodate different substrates or transition state structures.[56]

Synthesis. The synthesis of **2** was completed through a Suzuki reaction between **BrTPA**[51,54] (**4**) and 1,4-benzene diboronic acid (**5**) catalyzed by Pd(0) with 67% yield (Figure 1). For **3**, 1,3-benzene diboronic acid was obtained[57] first and esterified with pinacol in $CHCl_3$ to give 1,3-benzene diboronic acid dipinacol ester (**6**), which was easily purified by running through a silica plug. Compounds **4** and **6** were then reacted in 2:1 ratio in the presence of Pd(0) catalyst to give **3** in 85% yield.

The complex Zn_2(**2**)$(AN)_2(ClO_4)_4$ (**7**) was prepared by mixing **PBTPA** (**2**) and $Zn(ClO_4)_2$ in 1:2 ratio in MeOH and CH_3CN. Crystals suitable for X-ray diffraction were prepared by diffusing various volatile solvents into the CH_3CN solution of the complex. Colorless transparent crystals were obtained respectively with Et_2O, THF, EtOAc, and CH_2Cl_2 as diffusing solvents. The crystals prepared from Et_2O and THF yielded two different structures (**7a** and **7b**, respectively) determined by X-ray diffraction. Complex Cu_2(**2**)$(AN)_2(ClO_4)_4$ (**8**) was prepared by the same method, except that suitable crystals were only obtained when EtOAc was diffused into the CH_3CN solution of **8**. The crystals were formed as clusters (same phenomena were observed when other solvents were used without exception). The pleochroic crystals appeared either deep blue or pale violet as rotated around their long axis.

X-ray Structures. All the crystal data and structural refinements are summarized in Table 1. The X-ray structure of [Cu(**1**)(**BNPP**)](ClO_4) in Figure 2[58] shows that the Cu-

(56) Breslow, R. *Acc. Chem. Res.* **1995**, *28*, 146.
(57) Nielsen, D. R.; McEwen, W. E. *J. Am. Chem. Soc.* **1957**, *79*, 3081.
(58) Farrugia, L. J. *J. Appl. Crystallogr.* **1997**, *30*, 565.

Table 1. Crystal Data and Structure Refinements for [Cu(**1**)(**BNPP**)](ClO$_4$), [Zn$_2$(**2**)(AN)$_2$](ClO$_4$)$_4$ (**7a**, **7b**), and [Cu$_2$(**2**)(AN)$_2$(ClO$_4$)](ClO$_4$)$_3$ (**8**)

	[Cu(**1**)(**BNPP**)](ClO$_4$)	[Zn$_2$(**2**)(AN)$_2$](ClO$_4$)$_4$ (**7a**)	[Zn$_2$(**2**)(AN)$_2$](ClO$_4$)$_4$ (**7b**)	[Cu$_2$(**2**)(AN)$_2$(ClO$_4$)](ClO$_4$)$_3$ (**8**)
empirical formula	$C_{30}H_{26}ClCuN_6O_{12}P$	$C_{56}H_{63}Cl_4N_{13}O_{17}Zn_2$	$C_{52}H_{56}Cl_4N_{13}O_{16}Zn_2$	$C_{46}H_{44}Cu_2N_{10}Cl_4O_{16}$
fw	792.53	1462.73	1391.64	1261.79
temp	173(2) K	173(2) K	173(2) K	173(2) K
wavelength	0.71073 Å	0.71073 Å	0.71073 Å	0.71073 Å
crystal system	triclinic	monoclinic	monoclinic	monoclinic
space group	$P\bar{1}$	Cc	$P2_1/c$	$P2_1/c$
unit cell dimens	a = 9.0338(7) Å	a = 21.411(3) Å	a = 11.7208(12) Å	a = 14.652(2) Å
	b = 10.3878(8) Å	b = 11.106(2) Å	b = 18.3144(18) Å	b = 23.435(4) Å
	c = 17.567(1) Å	c = 29.054(4) Å	c = 14.1549(14) Å	c = 15.434(3) Å
	α = 90.969(1)°	α = 90°	α = 90°	α = 90°.
	β = 100.544(1)°	β = 111.138(2)°	β = 97.332(2)°	β = 109.384(4)°.
	γ = 100.361(1)°	γ = 90°	γ = 90°	γ = 90°.
volume	1592.1(2) Å^3	6443.7(15) Å^3	3013.6(5) Å^3	4999.1(14) Å^3
Z	2	4	2	4
density (calcd)	1.653 Mg/m^3	1.508 Mg/m^3	1.534 Mg/m^3	1.676 Mg/m^3
absorption coeff	0.897 mm^{-1}	0.988 mm^{-1}	1.051 mm^{-1}	1.148 mm^{-1}
F(000)	810	3016	1430	2576
crystal color, morphology	light blue, plate	colorless, block	colorless, block	blue/violet (pleochroic), plate
crystal size	0.38 × 0.32 × 0.16 mm^3	0.44 × 0.32 × 0.14 mm^3	0.30 × 0.25 × 0.13 mm^3	0.25 × 0.20 × 0.10 mm^3
θ range for data collection	1.18−27.53°	1.50−27.55°	1.75−25.04°	1.47−25.17°
index ranges	$-11 \le h \le 11$, $-13 \le k \le 13$, $-22 \le l \le 22$	$-27 \le h \le 27$, $-14 \le k \le 14$, $-37 \le l \le 37$	$-13 \le h \le 13$, $-21 \le k \le 21$, $-16 \le l \le 16$	$-17 \le h \le 16$, $0 \le k \le 27$, $0 \le l \le 18$
reflections collected	19166	37432	22569	56057
indep reflns	7254 [R(int) = 0.0180]	14738 [R(int) = 0.043]	5322 [R(int) = 0.037]	8946 [R(int) = 0.0647]
obsd reflns	6392	12099	4387	7024
completeness to θ = 27.53°	98.7%	99.6%	99.9%	99.6%
absorption correction	multiscans	multiscans	multiscans	multiscans
max and min transmission	1.000000 and 0.901804	0.869 and 0.755	0.864 and 0.764	0.8939 and 0.7623
refinement meth	full-matrix least-squares on F^2	full-matrix least-squares on F^2	full-matrix least-squares on F^2	full-matrix least-squares on F^2
data/restraints/params	7254/0/460	14738/2/706	5322/90/404	8946/0/707
GOF on F^2	1.019	1.026	1.063	1.057
final R indices [$I > 2\sigma(I)$]	$R1$ = 0.0295, $wR2$ = 0.0805	$R1$ = 0.0383, $wR2$ = 0.0873	$R1$ = 0.0481, $wR2$ = 0.1232	R1 = 0.0472, wR2 = 0.1157
R indices (all data)	$R1$ = 0.0352, $wR2$ = 0.0831	$R1$ = 0.0500, $wR2$ = 0.0924	$R1$ = 0.0604, $wR2$ = 0.1345	R1 = 0.0652, wR2 = 0.1270
largest diff peak and hole	0.421 and −0.534 e Å^{-3}	0.402 and −0.373 e Å^{-3}	0.753 and −0.684 e Å^{-3}	1.047 and −0.469 e Å^{-3}

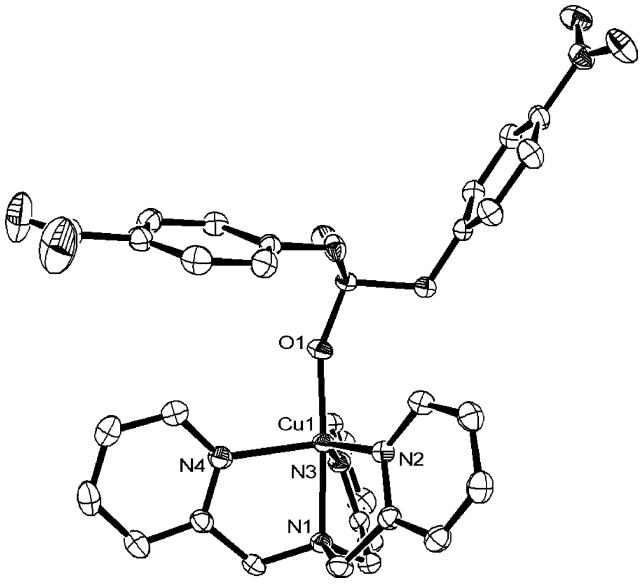

Figure 2. ORTEP diagram (50% probability ellipsoids) of the cationic portion of [Cu(**1**)(**BNPP**)](ClO$_4$). Hydrogen atoms are removed for clarity.

(II) center adopts a distorted trigonal bipyramidal geometry, where one of the nonesterified oxygen atoms O1 of **BNPP** occupies the apical position opposite to the tertiary nitrogen atom N1. The four Cu−N bond lengths fall in the range 2.02−2.15 Å; the bond length of Cu−O1 is 1.92 Å (Table 2). The coordination chemistry and the geometric data of

Table 2. Selected Bond Lengths (Å) and Angles (deg) of [Cu(**1**)(**BNPP**)](ClO$_4$)

Cu1−N1	2.0187(14)				
Cu1−N2	2.0406(15)	83.28(6)			
Cu1−N3	2.0258(15)	81.51(6)	132.48(6)		
Cu1−N4	2.1508(16)	80.31(6)	109.45(6)	111.86(6)	
Cu1−O1	1.9196(13)	174.27(6)	102.45(6)	94.40(6)	97.63(6)
		N1	N2	N3	N4

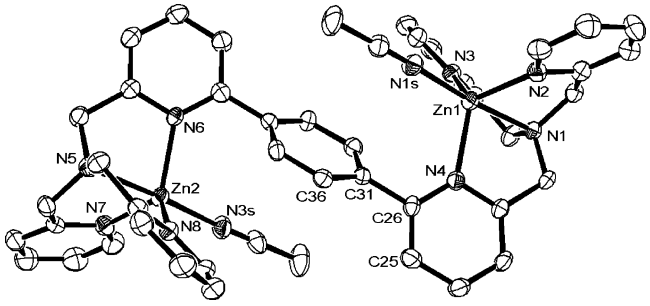

Figure 3. ORTEP diagram (50% probability ellipsoids) of cationic portion of [Zn$_2$(**2**)(AN)$_2$](ClO$_4$)$_4$ (**7a**). Hydrogen atoms are removed for clarity.

Cu(II) are almost identical to those of Zn(II) in the structure of [Zn(**1**){OP(O)(C$_6$H$_4$NO$_2$)O}Zn(**1**)](BPh$_4$)$_2$.[59] These structures suggest that both [Cu(II)(**TPA**)] and [Zn(II)(**TPA**)] would serve as valid phosphodiester binding motifs with similar binding modes.

(59) Adams, H.; Bailey, N. A.; Fenton, D. E.; He, Q.-Y. *J. Chem. Soc., Dalton Trans.* **1995**, 697.

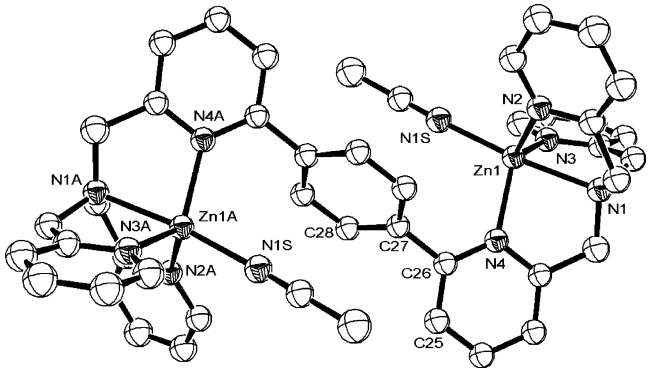

Figure 4. ORTEP diagram (50% probability ellipsoids) of cationic portion of $[Zn_2(\mathbf{2})(AN)_2](ClO_4)_4$ (**7b**). Hydrogen atoms are removed for clarity.

Table 3. Selected Bond Lengths (Å) and Bond Angles (deg) for **7a**, **7b**, and **8**

	$[Zn_2(\mathbf{2})(AN)_2](ClO_4)_4$ (**7a**)	$[Zn_2(\mathbf{2})(AN)_2](ClO_4)_4$ (**7b**)	$[Cu_2(\mathbf{2})(AN)_2(ClO_4)](ClO_4)_3$ (**8**)
		Bond Lengths	
M1−N1	2.166(3)	2.199(3)	2.026(3)
M1−N2	2.088(3)	2.036(3)	2.412(3)
M1−N3	2.051(3)	2.078(3)	1.992(3)
M1−N4	2.080(3)	2.085(3)	1.989(3)
		Bond Angles	
N1−**M1**−N2	78.07(11)	80.98(13)	83.18(11)
N1−**M1**−N3	79.84(11)	78.83(13)	82.14(12)
N1−**M1**−N4	78.88(11)	79.49(12)	82.50(12)
N2−**M1**−N3	120.98(11)	117.33(13)	85.16(11)
N2−**M1**−N4	116.84(11)	114.89(13)	95.63(11)
N3−**M1**−N4	111.31(10)	118.49(13)	164.42(13)

Both **7a** and **7b** (Figures 3 and 4) structures displayed distorted trigonal bipyramidal Zn(II) coordination geometry with similar bond lengths and angles in the coordination domains (Table 3). The ones grown from Et_2O (**7a**) crystallized in the space group *Cc*. Although there is evidence of a center of symmetry in the structure, the space group is almost certainly *Cc* and not *C*2/*c*. The main reason for this deduction is that when the structure is solved in *C*2/*c* the final *R* value is about 20%, some atoms display very poor anisotropic thermal displacement parameters, and there are areas of high residual difference electron density in nonsensical places. Another indicator is that the value of $|E2 - 1|$ is 0.77, i.e., close to that expected for non-centrosymmetric symmetry.

The crystals of **7a** have both Et_2O and CH_3CN in the lattice; however, the solvent molecules proved to be too disordered to be modeled satisfactorily so their associated electron density was removed from the structural refinement. The ones grown from THF (**7b**) crystallized in the space group $P2_1/c$. They have CH_3CN in the lattice but no THF. The solvent molecules were disordered but modeled satisfactorily in the structural refinement.

In structure **7a** (Figure 3), the distance between two metal ion centers (Zn1 and Zn2) is 8.350 Å. With the aid of a commercial software package (MacroModel),[60] the intermetal distances were measured as the dihedral angle C36−C31−C26−C25 (47.923° in the structure) was varied. The shortest intermetal distance that could be reached was 5.494 Å, which is close to the values reported in some bimetallonucleases.[61]

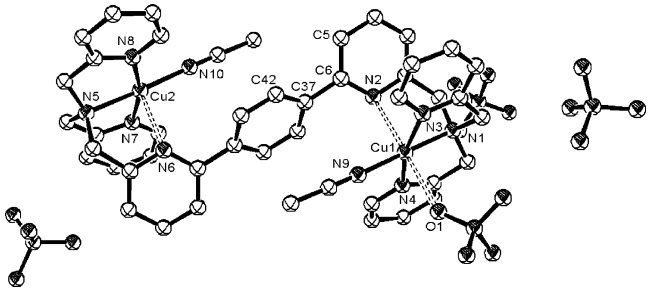

Figure 5. ORTEP diagram (50% probability ellipsoids) of $[Cu_2(\mathbf{2})(AN)_2(ClO_4)](ClO_4)_3$ (**8**). Hydrogen atoms are removed for clarity.

The intermetal distance (Zn1−Zn1A) in structure **7b** (Figure 4) is 8.305 Å. The dihedral angle C28−C27−C26−C25 (52.894° in the structure) was varied so that the shortest distance between two metal centers was 5.480 Å, comparable to that obtained in **7a**. It was observed that the dihedral angles between phenyl planes and the planes of the connecting pyridyl groups in **7a** and **7b** differed by 5°. Thus in structure **7b**, the plane of one pyridyl group in each [Zn(II)**TPA**] moiety was almost parallel to the phenyl plane, whereas in structure **7a** this correlation was not observed. The subtle difference from the two dihedral angles (which involved the only rotational freedom in the complex) may very well have contributed to the magnified difference in the crystal lattice packing to result in two distinct solid structures.

In the Cu(II) complex $[Cu_2(\mathbf{2})(AN)_2(ClO_4)](ClO_4)_3$ (**8**, Figure 5), the Cu(II) ions, three nitrogen atoms from **2**, and a nitrogen atom from CH_3CN form a square planar geometry, with the Cu−N bond lengths ranging from 1.98 to 2.02 Å (Table 3), in contrast to what was observed in the structure of [Cu(**1**)(**BNPP**)](ClO_4) and other documented Cu(II)−**TPA** structures.[62] The pyridyl nitrogen atom N2 and one oxygen atom (O1) from a perchlorate associate weakly with Cu(II) from the two apical positions. One perchlorate (Cl1) links Cu1 and Cu2 on adjacent tetracations. These Cu···O interactions are very long with Cu1−O1 = 2.621(4) Å and Cu2−O2#1 = 2.688(4) Å. These are at least 0.1 Å longer than the mean value for Cu(II) 5,6 coordinate structures, as listed in the *International Tables for Crystallography*, Vol. C, p 756. The nitrogen atoms from the *p*-di-2-pyridylbenzene backbone do not bond strongly, if at all, to their respective Cu atoms. Both are slightly longer than 2.4 Å and well outside normal pyridyl bonding distances. These pyridyl rings are also tilted 47.2° and 45.1° from the normal of the plane formed by the Cu atoms and the remaining three N atoms, respectively. The three perchlorate anions not involved in linking the tetracations are involved in a number of important weak C−H···O type hydrogen bonds.

The distance between two Cu(II) centers is 9.327 Å. By varying the dihedral angle C42−C37−C6−C5 (33.453° in

(60) Mohamadi, F.; Richards, N. G. J.; Guida, W. C.; Liskamp, R.; Lipton, M. C., C.; Chang, G.; Hendrickson, T.; Still, W. C. *J. Comput. Chem.* **1990**, *11*, 440.

(61) Kim, Y.; Eom, S. H.; Wang, J.; Lee, D.-S.; Suh, S. W.; Steitz, T. A. *Nature* **1995**, *376*, 612.

(62) Allen, C. S.; Chuang, C.-L.; Cornebise, M.; Canary, J. W. *Inorg. Chim. Acta* **1995**, *239*, 29.

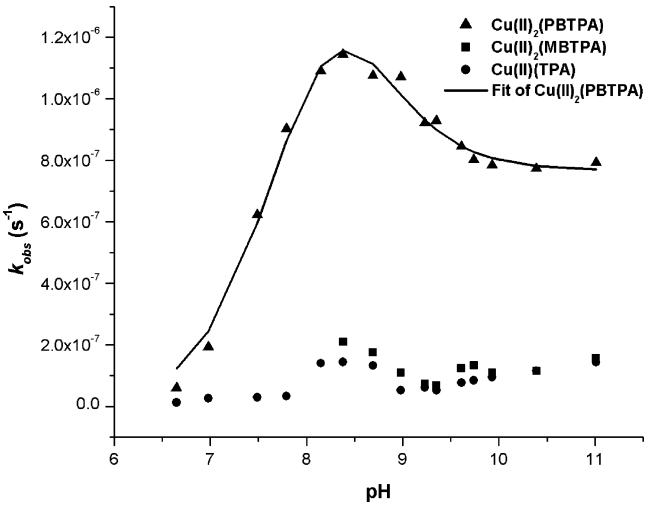

Figure 6. Plot of the observed rates of hydrolyses of **BNPP** (2.0 mM) catalyzed by Cu(II)$_2$(**2**) (▲, 0.20 mM, average of two runs), Cu(II)$_2$(**3**) (■, 0.20 mM), and Cu(II)(**1**) (●, 0.40 mM) at various pH values (0.05 M buffer solution containing 0.1 M $NaClO_4$) in 30% DMSO solution (v/v). The background rates in the absence of catalyst are subtracted. The solid line is a theoretical fit by eq 1.

the structure), the shortest distance 6.480 Å could be reached. However, since N6 and N2 do not bind, or bind very loosely, to respective Cu atoms, this structure has more rotational freedom than its Zn(II) counterpart. Therefore, even shorter intermetal distances might be allowed in the solution structures.

Hydrolysis of BNPP. In kinetic studies of **BNPP** hydrolysis probing the catalytic activity of the synthetic ligand−metal complexes, a concentrated solution of substrate **BNPP** (50 mM in DMSO), binuclear ligand (5.0 mM in DMSO), and $Cu(ClO_4)_2$ (10.0 mM in H_2O) were added sequentially with H_2O, DMSO, and buffer (0.1 M in H_2O in the presence of 0.2 M $NaClO_4$ for keeping ionic strength) to give a 30% DMSO solution. Final concentrations were 2.0 mM for **BNPP**, 0.20 mM for binuclear ligand, 0.40 mM for $Cu(ClO_4)_2$, and 0.05 M for buffer so that binuclear ligand would form 1:2 complex with Cu^{2+} in situ. Efficient metal binding under these conditions was expected,[50] and stable metal complex formation was confirmed by the absence of precipitation of metal hydroxide at high pH. The formation of hydrolysis product *p*-nitrophenol/*p*-nitrophenylate was monitored by absorbance at 400 nm. The observed first-order rate constants (k_{obs}) were calculated by the initial rate method. In determination of pH vs rate correlation of hydrolysis catalyzed by bimetallic catalysts, various buffer solutions (HEPES, pH < 8.0; EPPS, 8.0 < pH < 8.9; CHES, 8.9 < pH < 11.0; CAPS, pH > 11.0) were used to cover the pH region of interest.[25] A control experiment with mononuclear ligand **1** was also performed, in which **1** was added at twice the concentration of the binuclear ligands so that it would form 1:1 complex with Cu^{2+}.[50] The pH vs rate profiles are shown in Figure 6.

In complex Cu(II)$_2$(**2**) catalyzed **BNPP** hydrolysis, the pH vs rate correlation in Figure 6 is an unsymmetrical bell-shaped curve with a maximum observed first-order rate constant (k_{obs}) of 1.14×10^{-6} s^{-1} at pH ∼ 8.4, which is most likely between the two pK_as of the Cu(II)-bound water ligands in species **A** (Figure 7).[25] The solid curve is the theoretical plot constructed from eq 1[63] employing the second-order rate constants k_1, k_2, and k_3 for species **A**, **B**, and **C** and the appropriate pK_a values (Figure 7). It is presumed that **A**, **B**, and **C** are the only active catalytic species of Cu(II)$_2$(**2**) in solution.[64] At low pH where species **A** is dominant, there can be only Lewis acid activation of the phosphodiester substrate, which is far from enough to achieve significant enhancement,[2] and little acceleration of the hydrolysis is observed. Within pH range 8−9, the species **B** is abundant in which one Cu(II)-bound-water is deprotonated to generate an active nucleophile. As in the two-metal-ion mechanism proposed for a number of bimetallonucleases/phosphatases,[5] it is very likely that this species delivers a nucleophilic hydroxide to the phosphate center while the other metal ion is oriented to bind with the phosphoester moiety to provide Lewis acid activation. When all the geometric elements such as the intermetal distance are adjusted to give an energetically favorable complex between Cu(II)$_2$(**2**) and phosphodiester transition state structure, nucleophilic activation by one Cu(II) and Lewis acid activation by the other would participate in the process in a highly cooperative way to give more than the simple additive result of both activations, and a facile hydrolysis reaction is observed.[2] At pH 8.38 where Cu(II)$_2$(**2**) gives maximum enhancement, the rate of catalyzed hydrolysis is more than 10^4-fold over uncatalyzed reaction, and ∼10-fold over the reaction catalyzed by mononuclear catalyst Cu(II)(**1**).

$$k_{obs} = \frac{(k_1 a_H^{\ 2} + k_2 K_5 a_H + k_3 K_5 K_6)[\mathrm{Cu(II)_2(2)}]}{K_5 K_6 + K_5 a_H + a_H^{\ 2}} \qquad (1)$$

When pH becomes >9, the second Cu(II)-bound water is ionized, and the dominant species in solution is **C**. Species **C** has two tightly bound hydroxide ions at Cu(II) centers, which inhibit the coordination of the anionic phosphodiester substrate to the catalyst.[34,64] Although it is able to deliver two nucleophilic hydroxides, it lacks the cooperativity between two metal ion centers as in species **B**. Indeed, the enhancement of hydrolysis of **BNPP** by **C** is about 4 times less than the acceleration by **B**. (It is taken into account that **C** delivers twice as much nucleophile as **B**.)

The complex Cu(II)$_2$(**3**), however, did not significantly enhance the hydrolysis of **BNPP** as shown in Figure 6. Unlike the Cu(II)$_2$(**2**) containing reaction mixture, which was homogeneous at 55 °C throughout the reaction, Cu(II)$_2$(**3**) was difficult to dissolve under the same conditions, and therefore formed a slightly heterogeneous mixture. Nonetheless the kinetic measurements were conducted. The observed rate constants with $R^2 > 0.9$ were plotted in Figure 6. The k_{obs} values by Cu(II)$_2$(**3**) float around 1×10^{-7} s^{-1} independent of pH. CPK molecular models suggest that Cu(II)$_2$(**3**)

(63) Chin, J.; Banaszczyk, M.; Jubian, V.; Zou, X. *J. Am. Chem. Soc.* **1989**, *111*, 186.

(64) Another potential explanation for the loss of activity at higher pH could be reduction in the reaction order of the catalyst,[3] although related studies[51] indicated that similar complexes do not aggregate in aqueous solution.

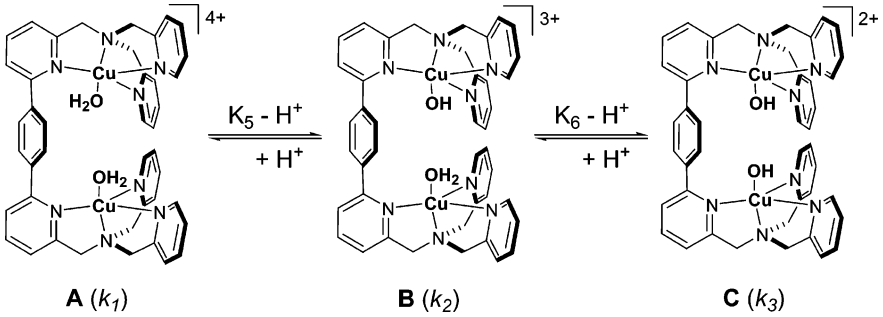

Figure 7. Species **A**, **B**, and **C** are presumed active species in catalyzing hydrolysis of **BNPP**. The second-order rate constants for each species are designated as k_1, k_2, and k_3, respectively. The theoretical fit of k_{obs} vs pH by eq 1 results in $k_1 \approx 0$; $k_2 = (8.3 \pm 0.7) \times 10^{-3}$ M^{-1} s^{-1}; $k_3 = (3.8 \pm 0.1) \times 10^{-3}$ M^{-1} s^{-1}; $K_5 = (1.8 \pm 0.3) \times 10^{-8}$ M; $K_6 = (2.5 \pm 0.9) \times 10^{-9}$ M.

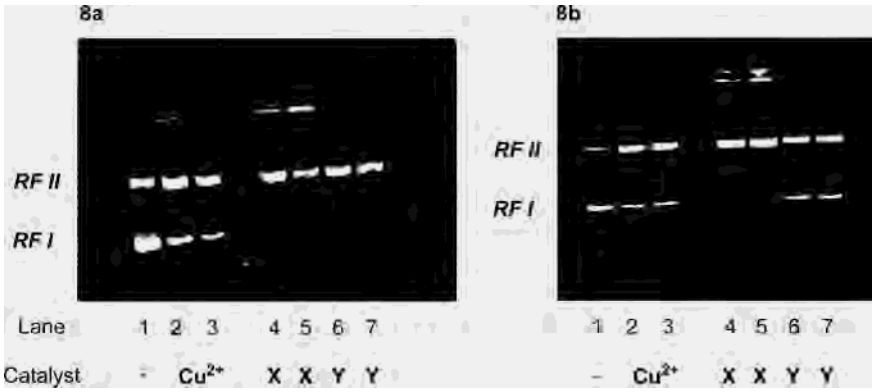

Figure 8. Electrophoretic separations of ϕX174 DNA (0.02 g/L) on 1% agarose gel followed cleavage with different catalysts (10.0 mM Cu(II) total concentration) in pH 8.75 (0.10 M CHES, 0.20 M $NaClO_4$) 30% DMSO solution (v/v) at 45 °C for 2 h. Catalyst **X**: $Cu(II)_2$(**2**). **Y**: Cu(II)(**1**). **8a**: experiment under aerobic conditions. **8b**: under anaerobic conditions.

has a shorter intermetal distance than $Cu(II)_2$(**2**) does, which might contribute to its ability to form species with atoms bridged between two Cu(II) centers, thus hampering its catalytic efficiency in **BNPP** hydrolysis.[22,23] The other probable explanation is that the two [Cu(II)**TPA**] domains that are *meta* to each other in $Cu(II)_2$(**3**) are unable to orient the two Cu(II) centers into positions relative to the substrate that are favorable for phosphoryl transfer reactions.[23]

The binuclear complex of Zn(II) and **PBTPA** was also tested for **BNPP** hydrolysis activity. Under identical conditions, the maximum first-order reaction rate 2.3×10^{-8} s^{-1} was observed at pH 8.2. It was about 100-fold slower than what was observed with binuclear Cu(II) complex. The bell-shaped pH vs rate profile characteristic of binuclear cooperativity was not observed. The difference between activities of Zn(II) and Cu(II) complexes must in part originate from the greater Lewis acidity of Cu(II). Additionally, the different coordination geometries observed between Zn(II) and Cu(II) complexes in the X-ray structures may reflect different solution structures between both complexes. The weakly bound third pyridyl group in the Cu(II) complex structure may provide additional rotational freedom, which the Zn(II) complex lacks, for binding the substrate in solution that would result in an energetically favorable transition state complex.

Hydrolysis of Phage ϕX174 DNA. A phage ϕX174 DNA assay was performed to study the DNA cleavage activity of $Cu(II)_2$(**2**). Figure 8a shows the agarose gel electrophoresis patterns for the cleavage of ϕX174 after treatment with Cu_nL (L = **2**, $n = 2$; L = **1**, $n = 1$) at pH 8.75 and 45 °C for 2 h in 30% DMSO solution. The complete conversion of form I (supercoiled) DNA to form II (nicked) was observed with either **2** (5.0 mM) or **1** (10.0 mM) as the ligand at 10.0 mM total Cu(II) concentration, whereas a significant amount of form I remained when only free Cu^{2+} was present (Figure 8a). The same experiment conducted with Zn(II) as the coordinating metal ion did not show catalytic advantage of binuclear complex over either Zn(II)−**TPA** mononuclear complex or free Zn(II) ion.

However, it is well-known that Cu(II) complexes promote oxidative nucleic acid strand scission through various pathways.[65−67] In cleavage and ligation reactions of DNA in nucleic acid biotechnology, they are preferred to be reversible transformations rather than the irreversible process that results from DNA oxidative cleavage.[3] In order to probe the hydrolytic activity of the Cu(II) complexes, an anaerobic assay was conducted under otherwise identical conditions (Figure 8b). The complete conversion of form I to form II was again observed with $Cu(II)_2$(**2**) as the catalyst. However, complex Cu(II)(**1**) and free Cu^{2+} ions showed similarly dismal activity in promoting hydrolytic supercoiled DNA relaxation. The percentages of form I and form II products obtained were semiquantified by densitometry, which showed that 96% supercoiled ϕX174 DNA was hydrolyzed to the

(65) Pogozelski, W. K.; Tullius, T. D. *Chem. Rev.* **1998**, *98*, 1089.
(66) Melvin, M. S.; Tomlinson, J. T.; Saluta, G. R.; Kucera, G. L.; Lindquist, N.; Manderville, R. A. *J. Am. Chem. Soc.* **2000**, *122*, 6333.
(67) Humphreys, K. J.; Karlin, K. D.; Rokita, S. E. *J. Am. Chem. Soc.* **2002**, *124*, 6009.

nicked form by binuclear Cu(II)$_2$(**2**) complex, whereas only 61% hydrolysis was achieved by Cu(II)(**1**), which essentially has the same activity as free Cu^{2+} ions. Therefore, the fact that relaxation of supercoiled (form I) DNA occurred under anaerobic conditions signifies that Cu(II)$_2$(**2**) cleaves DNA via a nonoxidative, hydrolytic pathway. Comparing Figure 8a with 8b, it is also noted that both Cu(II)$_2$(**2**) and Cu(II)(**1**) are able to cleave form I via an oxidative pathway. However, Cu(II)(**1**) did not enhance the *hydrolysis* over Cu^{2+} ion. The hydrolytic enhancement by participation of ligand **2** and the inactivity of complex Cu(II)(**1**) suggest that, in this particular case, the activity of Cu(II)$_2$(**2**) results from a bimetallic cooperative mechanism, not merely the additive result of two mononuclear metal binding units.

Conclusion

In summary, two isomeric homobinuclear ligands (**2**, **3**) designed to imitate the general active site structures of bimetallonucleases/phosphatases were prepared. Published metal-bound-water acidity data of $[M(\mathbf{1})(H_2O)]^{2+}$ (M = Zn(II) or Cu(II)) complexes[50] indicate that metal-bound hydroxide nucleophile would be provided in near neutral water; the X-ray structure of [Cu(**1**)(**BNPP**)](ClO_4) shows that [Cu(**1**)]$^{2+}$ complex binds with the phosphodiester model compound **BNPP** in a mode similar to what was observed in numerous enzyme active sites. The X-ray structures of coordination complexes $[Zn_2(\mathbf{2})(AN)_2](ClO_4)_4$ (**7a**, **7b**) and $[Cu_2(\mathbf{2})(AN)_2(ClO_4)](ClO_4)_3$ (**8**) were examined. The Zn(II) centers in **7a** and **7b** adopt a distorted trigonal bipyramidal geometry, whereas each Cu(II) domain in **8** is square planar with a perchlorate oxygen atom and a pyridyl nitrogen atom loosely bound in apical positions. It was proved that the intermetal distances between two metal centers in all the structures could reach within 5.5 Å of each other, assuming only two degrees of rotational freedom (the C−C bonds between phenyl rings and the connecting pyridyl groups). The distances could very well be even shorter if more rotational freedom was allowed, which is apparent in the structure of $[Cu_2(\mathbf{2})(AN)_2(ClO_4)](ClO_4)_3$ (**8**).

The two isomeric binuclear ligands **2** and **3** differ only from the relative orientations of two metal binding sites with respect to each other. Yet we observed drastic differences in their catalytic efficiencies in hydrolyzing **BNPP**, a phosphodiester model compound. Complex Cu(II)$_2$(**2**) displayed greater activity toward catalyzing **BNPP** hydrolysis than Cu(II)$_2$(**3**) and mononuclear complex Cu(II)(**1**). At pH 8.4, the achieved rate enhancement by Cu(II)$_2$(**2**) for **BNPP** hydrolysis is $>10^4$. The fact that binuclear Cu(II)$_2$(**2**) is a much better catalyst than mononuclear Cu(II)(**1**) and its observed bell-shaped pH vs rate profile are in agreement with the two-metal-ion mechanism proposed for some bimetallonucleases/phosphatases.[5] The inactivity of Cu(II)$_2$(**3**) compared to Cu(II)$_2$(**2**) underscores the subtlety in the biomimetic design of effective catalysts. Furthermore, the ϕX174 RFI DNA assay demonstrated that catalyst Cu(II)$_2$(**2**) had much greater activity toward *hydrolyzing* phage ϕX174 RFI DNA than Cu(II)(**1**), a mononuclear Cu(II) complex. This study shows that binuclear complex Cu(II)$_2$(**2**) does not merely double the activity of its mononuclear counterpart. It supplies evidence for the two-metal-ion enzymatic mechanism by achieving cooperativity between two metal ions in this particular model system.

Acknowledgment. We thank William W. Brennessel, Dr. Neil R. Brooks, and Dr. Victor G. Young, Jr. in the X-Ray Crystallographic Laboratory, Department of Chemistry, University of Minnesota, for obtaining X-ray crystallographic data. FAB mass spectra were obtained at the Michigan State University Mass Spectrometry Facility. This work was supported by the NSF (CHE-0316589). O.S. acknowledges a NIH minority predoctoral fellowship.

Supporting Information Available: Derivation of eq 1 (PDF); X-ray crystallographic files for [Cu(**BNPP**)(**TPA**)](ClO_4), [Zn_2(**PBTPA**)$(AN)_2$](ClO_4)$_4$, and $[Cu_2(\mathbf{PBTPA})(AN)_2(ClO_4)](ClO_4)_3$ in CIF format. This material is available free of charge via the Internet at http://pubs.acs.org.

IC0340985